MODELING AND OPTIMIZATION OF THE AIR- AND GAS-SUPPLYING NETWORK OF A CHEMICAL PLANT

IN-SU HAN[a], CHONGHUN HAN[b] and CHANG-BOCK CHUNG[c]

[a] Department of Chemical Engineering, Pohang University of Science and Technology, Kyungbuk, Korea

[b] School of Chemical Engineering, Seoul National University, Seoul, Korea

[c] Faculty of Chemical Engineering, Chonnam National University, Gwangju, Korea

Abstract: This paper presents a novel optimization method for the air- and gas-supplying network comprised of several air compression systems and air and gas streams in an industrial chemical plant. The optimization is based on the hybrid model developed by Han and Han[1] for predicting the power consumption of a compression system. A constrained optimization problem was formulated to minimize the total electric power consumption of all the compression systems in the air- and gas-supplying network under various operating constraints and was solved using a successive quadratic optimization algorithm. The optimization approach was applied to an industrial terephthalic acid manufacturing plant to achieve about 10% reduction in the total electric power consumption under varying ambient conditions.

Keywords: Hybrid Modeling, Optimization, Air Compression System, Utility Plant, Partial Least-Squares.

1. INTRODUCTION

Air is one of the essential utilities for operating chemical plants and is usually supplied by compressors of various types. Typically, the compressor is connected with a steam turbine, a gas expander, or an electric motor as drivers on a single rotor, thus constitutes a compression system together with other auxiliary components such as bearings, coolers, and gears.[2] For a large-scale chemical plant, the compression systems are interconnected to each other to form a complex air-and gas-supplying network. In some cases, such a network consumes a major portion of the electric power spent in the plant, e.g., about 75 - 85 percent for a terephthalic acid(TPA) manufacturing plant.[3] Since the performances of the compressors strongly depend on process operating conditions and are different from each other, a considerable amount of energy can be saved by optimally operating the air- and gas-supplying network.[4]

Many optimization studies have been carried out for the utility systems in chemical plants, but most of them have been focused on steam production networks rather than air- or gas-supplying systems.[5-8] In industry, compressors and turbines are usually optimized on the basis of macroscopic mass and energy balances where the performances (efficiencies) of compressors and turbines are assumed to be constant or expressed as relatively simple correlations that fit the design diagrams.[9, 10] These industrial practices may not lead to the true optimal conditions because the performances of industrial compression systems are affected by diverse operating conditions such as discharge flow rate, ambient temperature and humidity, pressure drop through an air filter, compressor blade fouling, gas composition, and so forth.[4, 9]

This paper presents a novel optimization approach for the air- and gas-supplying network as well as its outcome when applied to the TPA manufacturing plant of Samsung Petrochemical Corporation in Ulsan, Korea. This work is based on and logically follows from the modeling study for the compression systems by Han and Han[1]. First, we present brief descriptions of the supplying network and the modeling procedure for the compression systems. Then, the optimization problem is formulated on the basis of the hybrid models and the mass balances on the network. Finally, the results of field application is presented and discussed.

Table 1. Configuration of the Compression Systems

Compression System	Number of Compression Stages	Number of Expansion Stages	Number of Electric Motors
Comp 1 (k = 1)	3	2	1
Comp 2 (k = 2)	4	2	1
Comp 3 (k = 3)	4	2	1
Comp 4 (k = 4)	4	2	1
Comp 5 (k = 5)	4	0	1

2. DESCRIPTION OF THE AIR- AND GAS-SUPPLYING NETWORK

Figure 1 shows a schematic diagram of the air-compression system consisting of a multistage compressor, an electric motor, and a multistage expander in the air- and gas-supplying network of a chemical plant. The compressor consists of several compression stages in series with an intercooler installed between successive compression stages. Humid air enters the suction of the first compression stage and is pressurized up to a desired level through several stages.

Table 2. Variables Used for the Hybrid Modeling of the Compression Systems

Compression System	$\mathbf{x}_1^{(k)}$ (Manipulated Variables)	$\mathbf{x}_2^{(k)}$ (Unknown Operating Variables)	$\mathbf{x}_3^{(k)}$ (Ambient Conditions)
Comp 1 (k=1)	$F_{a(3)}^{(1)}$, $F_{g(1)}^{(1)}$, $P_{ad(3)}^{(1)}$, $P_{gp(1)}^{(1)}$, $T_{gp(1)}^{(1)}$, $T_{gp(2)}^{(1)}$	$T_{ad(3)}^{(1)}$, $\phi_C^{(1)}$	T_e, H_a, $\lambda_{O2}^{(1)}$, $\lambda_{CO2}^{(1)}$, $\lambda_{CO}^{(1)}$
Comp 2 (k=2)	$F_{a(4)}^{(2)}$, $F_{g(1)}^{(2)}$, $P_{ad(4)}^{(2)}$, $P_{gp(1)}^{(2)}$, $T_{gp(1)}^{(2)}$, $T_{gp(2)}^{(2)}$	$T_{ad(4)}^{(2)}$, $\phi_C^{(2)}$, $\Delta P_F^{(2)}$	T_e, H_a, $\lambda_{O2}^{(2)}$, $\lambda_{CO2}^{(2)}$, $\lambda_{CO}^{(2)}$
Comp 3 (k=3)	$F_{a(4)}^{(3)}$, $F_{g(1)}^{(3)}$, $P_{ad(4)}^{(3)}$, $P_{gp(1)}^{(3)}$, $T_{gp(1)}^{(3)}$, $T_{gp(2)}^{(3)}$	$T_{ad(4)}^{(3)}$, $\phi_C^{(3)}$, $\phi_E^{(3)}$, $\Delta P_F^{(3)}$, $S_{E(1)}^{(3)}$, $S_{E(2)}^{(3)}$	T_e, H_a, $\lambda_{O2}^{(3)}$, $\lambda_{CO2}^{(3)}$, $\lambda_{CO}^{(3)}$
Comp 4 (k=4)	$F_{a(4)}^{(4)}$, $F_{g(1)}^{(4)}$, $P_{ad(4)}^{(4)}$, $P_{gp(1)}^{(4)}$, $T_{gp(1)}^{(4)}$, $T_{gp(2)}^{(4)}$	$T_{ad(4)}^{(4)}$, $\phi_C^{(4)}$, $\phi_E^{(4)}$, $\Delta P_F^{(4)}$, $S_{E(1)}^{(4)}$, $S_{E(2)}^{(4)}$	T_e, H_a, $\lambda_{O2}^{(4)}$, $\lambda_{CO2}^{(4)}$, $\lambda_{CO}^{(4)}$
Comp 5 (k=5)	$F_{a(4)}^{(5)}$, $P_{ad(4)}^{(5)}$	$T_{ad(4)}^{(5)}$, $\phi_C^{(5)}$, $\Delta P_F^{(5)}$	T_e, H_a

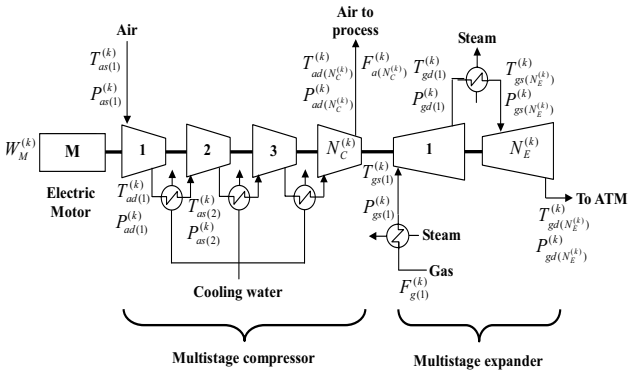

Figure 1. Schematic of the multistage air-compression system

Because an isothermal compression process requires the minimum power, the intercooler lowers the temperature of the air discharged from each stage. The expander is used as the primary driver of the compressor and is comprised of several expansion stages in series with a re-heater installed in-between to maximize the energy recovery. The electric motor makes up for the deficient portion of the total power requirement of the compression system which the expander cannot provides.

Figure 2 shows the air- and gas-supplying network comprised of the five compression systems and the air and gas streams in the TPA manufacturing plant of Samsung Petrochemical Corporation in Ulsan, Korea. Table 1 lists the configuration of the compression systems in the network. The compressor of each compression system provides the compressed air to various users such as the p-Xylene oxidizers, the TPA crystallizers, and the instrumental air units. The oxidizers are the main users oxidizers are the main users that take up about 90 percent of the total compressed air. The inert high-pressure nitrogen is recovered from the oxidizers along with some by-product gases. This off-gas is supplied for the pneumatic conveying of particles and the driving of the expanders through the interconnected gas-stream lines. The flow rates and pressures of the air and off-gas are kept regulated and balanced throughout the network by the control systems.

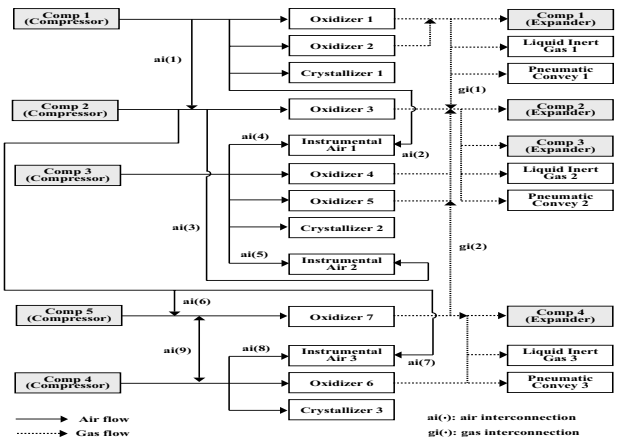

Figure 2. Air- and gas-supplying network of the TPA plant

3. MODELING OF THE COMPRESSION SYSTEMS

In this section we will only briefly outline the modeling approach for the compression systems in the network and refer the readers to the paper by Han and Han1 for the details. Figure 3 depicts the prediction procedure for the electric power consumption $W_M^{(k)}$ of the k-th compression system in the air- and gas-supplying network. $W_M^{(k)}$ is ultimately calculated using the thermodynamic equation

$$W_M^{(k)} = (W_{C0}^{(k)} + W_{E0}^{(k)})/\eta_O^{(k)}, \qquad k = 1, 2, \cdots, N_S \tag{1}$$

where $W_{C0}^{(k)}$ and $W_{E0}^{(k)}$ are the minimum and maximum powers of all the compression stages and expansion stages, respectively, that can be theoretically obtained under adiabatic and reversible conditions by

$$W_{C0}^{(k)} = \frac{\gamma_a^{(k)} \widetilde{F}_a^{(k)} R T_e N_C^{(k)}}{(\gamma_a^{(k)} - 1) M_{wa}} \left[\left(\frac{P_{ad(N_C^{(k)})}^{(k)}}{P_e} \right)^{\frac{\gamma_a^{(k)}-1}{N_C^{(k)} \gamma_a^{(k)}}} - 1 \right], \quad k = 1, 2, \cdots, N_S \tag{2}$$

$$W_{E0}^{(k)} = \frac{\gamma_g^{(k)} F_{g(1)}^{(k)} R T_{gs(1)}^{(k)} N_E^{(k)}}{(\gamma_g^{(k)} - 1) M_{wg}^{(k)}} \left[\left(\frac{P_e}{P_{gs(1)}^{(k)}} \right)^{\frac{\gamma_g^{(k)}-1}{N_E^{(k)} \gamma_g^{(k)}}} - 1 \right], \quad k = 1, 2, \cdots, N_S \tag{3}$$

and $\eta_O^{(k)}$ is the overall efficiency that colligates the performances of all the components comprising the compression system and is to be predicted as a function of operating variables and ambient conditions. The variables affecting $\eta_O^{(k)}$ are classified into three categories: 1) the manipulated variables $\mathbf{x}_1^{(k)}$ that can be set by the operator, 2) the unknown state variables $\mathbf{x}_2^{(k)}$ that vary with other operating variables, and 3) the ambient conditions $\mathbf{x}_3^{(k)}$. Table 2 lists the classified variables for each of the five compression systems in the network. The partial least squares (PLS) models[11] are constructed for the prediction of the unknown variables and efficiency, respectively, on the basis of the operating data for the past nine months, and are combined with the thermodynamic equations (1)-(3) to form a hybrid model for predicting the actual power consumption. The typical performance of the hybrid model is demonstrated by Figure 4 that shows excellent agreement between the measured and predicted values of the electric power consumption for Comp 1 with 0.69% average prediction error. Similar performances were obtained for the other compression systems with the average errors ranging between 0.49% and 1.25%.

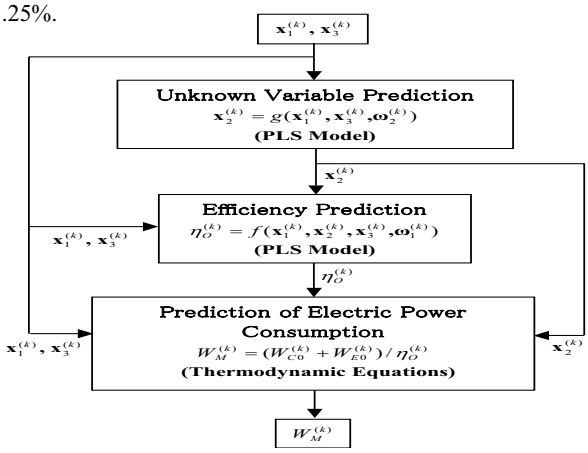

Figure 3. Prediction procedure of the electric power consumption of the kth compression system

4. FORMULATION OF THE OPTIMIZATION PROBLEM

The objective of the optimization is to minimize the total electric power consumption of all the compression systems in the air- and gas-supplying network under various operating constraints. The objective is achieved by formally solving the following constrained optimization problem:

$$\min_{\mathbf{X}_1} J = \sum_{k=1}^{N_S} W_M^{(k)} = \sum_{k=1}^{N_S} [W_{C0}^{(k)} + W_{E0}^{(k)}] / \eta_O^{(k)} \tag{4}$$

subject to

$$\mathbf{A}\mathbf{X}_1 = \mathbf{b} \tag{5}$$

$$\mathbf{X}_{1,L} \le \mathbf{X}_1 \le \mathbf{X}_{1,U} \tag{6}$$

$$\mathbf{X}_{2,L} \le \mathbf{X}_2 \le \mathbf{X}_{2,U} \tag{7}$$

$$W_{M,L}^{(k)} \le W_M^{(k)} \le W_{M,U}^{(k)}, \quad k = 1, 2, \cdots, N_S \tag{8}$$

$$P_{ad(N_C^{(k)})}^{(k)} \le F_{a(N_C^{(k)})}^{(k)} \alpha_{C1}^{(k)} + \beta_{C1}^{(k)}, \quad k = 1, 2, \cdots, N_S \tag{9}$$

$$P_{ad(N_C^{(k)})}^{(k)} \ge F_{a(N_C^{(k)})}^{(k)} \alpha_{C2}^{(k)} + \beta_{C2}^{(k)}, \quad k = 1, 2, \cdots, N_S \tag{10}$$

$$P_{gs(1)}^{(k)} \le F_{g(1)}^{(k)} \alpha_{E1}^{(k)} + \beta_{E1}^{(k)}, \quad k = 1, 2, \cdots, N_S \tag{11}$$

$$P_{gs(1)}^{(k)} \ge F_{g(1)}^{(k)} \alpha_{E2}^{(k)} + \beta_{E2}^{(k)}, \quad k = 1, 2, \cdots, N_S \tag{12}$$

In the above, $\mathbf{X}_1$ denotes the vector of the optimization (decision) variables to be determined. It consists of most of the manipulated variables for all the compression systems (except the discharge pressures of the compressed air and the suction pressures of the off-gas which are predetermined by the operating conditions of the users) and the flow rates of the air and gas streams in the network. The equality constraint (5) represents the mass balances that allocate the air and gas streams to meet the demands of various users in the network. Equations (6) and (7) represent the lower and upper bounds on the optimization variables $\mathbf{X}_1$ and the other operating variables $\mathbf{X}_2$, which are imposed by hardware constraints, operating conditions, and safety considerations. Equation (8) confines the power loads of the electric motors between appropriate bounds. Equations (9) and (10) address the important safety limits in the operation of a compressor and prevent each compressor from being operated below a surge line and above a stonewall (or choke) line, respectively.12 The parameters $\alpha_{C1}^{(k)}$, $\alpha_{C2}^{(k)}$, $\beta_{C1}^{(k)}$, and $\beta_{C2}^{(k)}$ in the equations can be obtained from the performance curves of compressors provided by vendors. Equations (11) and (12) address the similar safety considerations for the expanders. Tables 3 and 4 list the optimization variables and various bounds explained in the above.

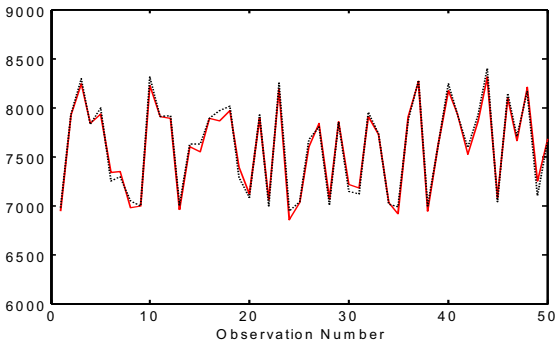

Figure 4. Comparison of the measured (dotted lines) and predicted (solid lines) values of the electric power consumption of Comp 1.

Table 3. Optimization (Decision) Variables and Their Operating Ranges

Variable Number	Optimization Variable	Lower Bound	Upper Bound	Variable Number	Optimization Variable	Lower Bound	Upper Bound
1	$F_{a(3)}^{(1)}$	17.8	29.0	15	$F_{g(1)}^{(1)}$	7.0	18.0
2	$F_{a(4)}^{(2)}$	13.0	27.0	16	$F_{g(1)}^{(2)}$	5.0	24.0
3	$F_{a(4)}^{(3)}$	14.5	34.0	17	$F_{g(1)}^{(3)}$	7.0	31.0
4	$F_{a(4)}^{(4)}$	12.5	35.5	18	$F_{g(1)}^{(4)}$	6.0	26.5
5	$F_{a(4)}^{(5)}$	8.0	14.0	19	$F_{g(1)}$	0	20.0
6	$F_{a(1)}$	0	25.0	20	$F_{g(2)}$	0	35.0
7	$F_{a(2)}$	0	3.0	21	$T_{g(1)}^{(1)}$	409.0	415.0
8	$F_{a(3)}$	0	3.0	22	$T_{g(1)}^{(2)}$	400.0	425.0
9	$F_{a(4)}$	0	3.0	23	$T_{g(1)}^{(3)}$	405.0	425.0
10	$F_{a(5)}$	0	3.0	24	$T_{g(1)}^{(4)}$	408.0	417.0
11	$F_{a(6)}$	0	9.0	25	$T_{g(2)}^{(1)}$	412.0	417.0
12	$F_{a(7)}$	0	3.0	26	$T_{g(2)}^{(2)}$	412.0	416.0
13	$F_{a(8)}$	0	3.0	27	$T_{g(2)}^{(3)}$	395.0	412.0
14	$F_{a(9)}$	-28.0	28.0	28	$T_{g(2)}^{(4)}$	418.0	428.0

5. RESULTS AND DISCUSSION

The optimization problem defined in Equations (4) – (12) is a nonlinear programming (NLP) problem. In this study, a successive quadratic programming (SQP) algorithm[13] was employed to solve this NLP problem. All the equations in the hybrid model are described in the objective function routine of the SQP algorithm. Since the optimization is performed on the basis of an open-equation approach, the solutions and optimization results are simultaneously found, and the

Table 4. Parameters of the Operating Bounds

Parameters	Comp 1 (k=1)	Comp 2 (k=2)	Comp 3 (k=3)	Comp 4 (k=4)	Comp 5 (k=5)
$W_{M,L}^{(k)}$	5850	7150	6100	4700	3600
$W_{M,U}^{(k)}$	10300	10300	12400	12596	7288
$\alpha_{C1}^{(k)}$	160.9	381.6	66.3	43.5	169.3
$\beta_{C1}^{(k)}$	-662.9	-6600.0	442.3	556.0	-65.1
$\alpha_{C2}^{(k)}$	16.9	84.1	9.2	10.0	18.9
$\beta_{C2}^{(k)}$	371.5	-1282.0	0.0	175.5	-98.1
$\alpha_{E1}^{(k)}$	108.0	71.3	81.9	67.5	-
$\beta_{E1}^{(k)}$	260.0	52.5	35.0	55.0	-
$\alpha_{E2}^{(k)}$	30.8	20.0	39.4	36.4	-
$\beta_{E2}^{(k)}$	846.0	280.0	57.1	101.6	-

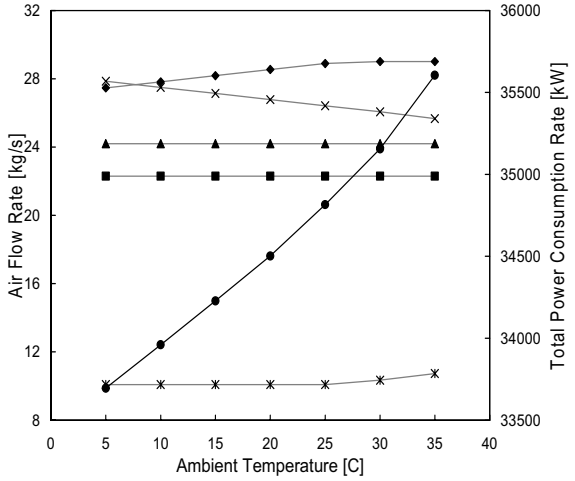

Figure 5. Effect of the ambient temperature on the optimization results

optimization model is more reproducible and needs lower maintenance cost than closed-equation approaches.[14] Fortran 90 codes were prepared for the optimization engine and the graphic user interface was constructed using Microsoft Visual BasicTM programming for field installation. Since the function evaluation in the optimization algorithm does not take much time, the optimization results were typically obtained within three seconds on a Pentium III-866 machine.

The optimization runs were carried out for the air- and gas-supplying network, depicted in Figure 2, in the TPA plant of Samsung Petrochemical Corporation using the optimization variables and their associated bounds listed in Tables 3 and 4. Since the ambient conditions listed in Table 2 represent the disturbance variables in the operation of the compression systems, their effects on the optimization results were investigated. Among the ambient conditions, the off-gas composition varies little due to stable composition control in the oxidizers, thus can be ignored in the optimization. On the other hand, since the ambient temperature and relative humidity change significantly between day and night as well as according to the seasonal and weather variations, they are regarded as the two major disturbance variables whose effects on the power consumption are to be examined in this study.

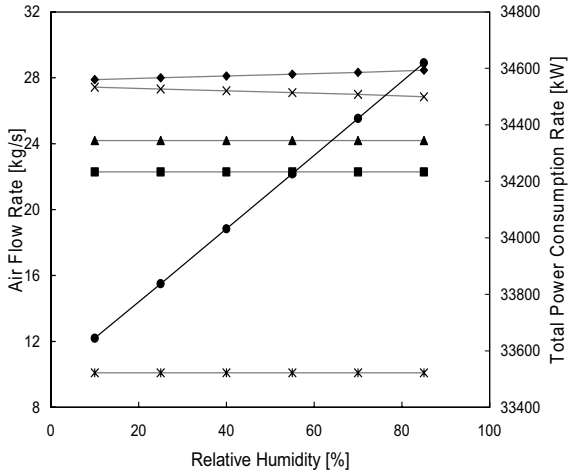

Figure 6. Effect of the relative humidity on the optimization results

Table 5. Optimization Variables before and after Optimization

Variable Number	Daytime Operation*		Nighttime Operation*	
	Before Optimization	After Optimization	Before Optimization	After Optimization
1	26.5	29.0	26.3	28.7
2	23.0	22.3	23.0	22.3
3	24.2	24.2	24.2	24.2
4	28.4	26.2	28.6	26.7
5	9.8	10.2	9.9	10.1
6	0.0	0.0	0.0	0.0
7	1.3	1.3	1.3	1.3
8	0.9	0.9	0.9	0.9
9	0.0	0.0	0.0	0.0
10	0.0	0.0	0.0	0.0
11	7.7	8.9	7.7	9.1
12	0.0	0.8	0.0	0.3
13	0.8	0.0	0.8	0.5
14	0.0	-1.4	0.0	-1.6
15	14.4	9.9	14.3	9.9
16	18.2	14.3	18.0	14.4
17	17.7	20.1	17.6	19.8
18	17.2	23.2	17.1	22.9
19	1.6	6.1	1.6	6.1
20	7.5	1.5	7.5	1.6
21	413.0	409.0	413.0	409.0
22	424.0	425.0	424.5	425.0
23	407.0	405.0	407.0	405.0
24	416.0	408.0	416.0	408.0
25	416.0	417.0	416.0	417.0
26	413.0	412.0	413.0	412.0
27	398.0	412.0	398.0	412.0
28	427.0	428.0	427.0	428.0

* The optimization results for the daytime operation was obtained at T_e = 299.5 K and H_a = 59 %, and those for the nighttime operation at T_e = 288.0 K and H_a = 71 %

Figure 5 shows the effect of the ambient temperature on the optimized power consumptions. The total power consumption at each optimal operating condition steadily increases with the rising ambient temperature, requiring about 1900kW (equivalent to about 5.7 percent) more power at the ambient temperature of 308 K than at 278 K. Figure 5 also shows that the optimal air flow rates are to be adjusted among the compression systems as the ambient temperature changes. Figure 6 shows a similar but slightly less sensitive effect that the relative humidity has on the optimized power consumptions. These optimization results demonstrate the necessity to adjust the operating conditions of the compression systems when there are considerable changes in the ambient temperature and relative humidity.

Compression System		Daytime Operation		Nighttime Operation	
		Before Optimization	After Optimization	Before Optimization	After Optimization
Comp 1	$\eta_O^{(1)}$	0.439	0.635	0.404	0.597
(k=1)	$W_M^{(1)}$	9577.4	9676.8	9438.9	9503.9
Comp 2	$\eta_O^{(2)}$	0.265	0.366	0.244	0.337
(k=2)	$W_M^{(2)}$	9170.5	8512.3	9082.5	8417.7
Comp 3	$\eta_O^{(3)}$	0.390	0.335	0.356	0.305
(k=3)	$W_M^{(3)}$	7580.2	7007.8	7557.9	6981.5
Comp 4	$\eta_O^{(4)}$	0.446	0.315	0.418	0.294
(k=4)	$W_M^{(4)}$	7789.5	4702.2	7748.7	4702.3
Comp 5	$\eta_O^{(5)}$	0.530	0.535	0.508	0.511
(k=5)	$W_M^{(5)}$	4949.8	5061.7	4964.9	5040.5
$\sum_{k=1}^{5} W_M^{(k)}$		39067.4	34960.8	38792.8	34645.9
Total Electric Power Reduced, (Percent Saved)		-	4106.6 (10.5)	-	4146.9 (10.7)

Table 6. Electric Power Consumptions before and after Optimization

Tables 5 and 6 compare the operating conditions and the electric power consumptions between before and after optimization. The optimizations were performed for two different sets of ambient conditions: the daytime operation (T_e = 299.5 K, H_a = 59 %) and the nighttime operation (T_e = 288.0 K, H_a = 71 %). Table 5 shows that the air and off-gas flow rates (F_a and F_g) should be reallocated to the compression systems and the off-gas temperatures (T_{gs}) should be adjusted from the present operating conditions to reduce the total electric power usage at each operation mode. Table 6 demonstrates that such changes of operating conditions led to about 10% reduction in the total power consumption both for the day and night operations.

NOMENCLATURE

F_a = flow rate of the air through a compression stage [kg/s]

F_{ai} = flow rate of the air through an inter connected line [kg/s]

$\widetilde{F}_a$ = average flow rate of the air through a multistage compressor [kg/s]

F_g = flow rate of the gas through an expansion stage [kg/s]

F_{gi} = flow rate of the gas through an interconnected line [kg/s]

H_a = relative humidity [%]

M_{wa} = average molecular weight of ambient air [kg/kg-mole]

M_{wg} = average molecular weight of the gas entering an expander [kg/kg-mole]

N_C = total number of compression stages of a compression system

N_E = total number of expansion stages of a compression system

N_S = total number of compression systems installed in the air- and gas-supplying network

P_{ad} = discharge pressure of the air from a compression stage [kPa]

P_{as} = suction pressure of the air at to compression stage [kPa]

P_e = atmospheric pressure [kPa]

P_{gd} = discharge pressure of the gas from an expansion stage [kPa]

P_{gs} = suction pressure of the gas to an expansion stage [kPa]

R = universal gas constant [8.314 kJ/kg-mole-K]

S_E = impeller rotating speed of a single expansion stage [RPM]

T_e = ambient temperature of compression systems [K]

T_{ad} = discharge temperature of the air from a compression stage [K]

T_{gs} = suction temperature of the gas to an expansion stage [K]

W_{C0} = minimum power required for a multistage compressor under an adiabatic and reversible process [kW]

W_{E0} = maximum power generated by a multistage expander under an adiabatic and reversible process [kW]

W_M = electric power delivered to an electric motor [kW]

$\mathbf{X}_1$ = vector of optimization (manipulated) variables for the air- and gas-supplying network

$\mathbf{x}_1$ = vector of manipulated variables of a compression system

$\mathbf{X}_2$ = vector of unknown operating variables in the air- and gas-supplying network, $\mathbf{X}_2 \in \{\mathbf{x}_2^{(k)} \mid k = 1, 2, \cdots N_S\}$

$\mathbf{x}_2$ = vector of unknown operating variables of a compression system

$\mathbf{x}_3$ = vector of ambient conditions of a compression system

Greek Letters

α_{C1} = slope of the surge control line of a compressor [kPa-s/kg]

α_{C2} = slop of the stonewall line of a compressor [kPa-s/kg]

α_{E1} = slope of the upper operation line of an expander [kPa-s/kg]

α_{E2} = slop of the lower operation line of an expander [kPa-s/kg]

β_{C1} = intercept of the surge control line of a compressor [kPa]

β_{C2} = intercept of the stonewall line of a compressor [kPa]

β_{E1} = intercept of the upper operation line of an expander [kPa]

β_{E2} = intercept of the lower operation line of an expander [kPa]

γ_a = average adiabatic exponent of the air through a multistage compressor

γ_g = average adiabatic exponent of the gas through a multistage expander

ΔP_F = pressure drop through a compressor filter [kPa]

η_O = overall efficiency of a compression system [0 – 1]

λ = weight fraction of gas [0 – 1]

ϕ_C = position of the inlet guide vane of a compressor [degree]

ϕ_E = position of the inlet guide vane of an expander [degree]

$\boldsymbol{\omega}_1$ = regression coefficient vector of the PLS model for the overall efficiency prediction

$\boldsymbol{\omega}_2$ = regression coefficient vector of the PLS model for the unknown variable prediction

Subscripts

a = air

C = compressor or compression stage

CO = carbon monoxide

$CO2$ = carbon dioxide

E = expander or expansion stage

e = ambient condition

g = gas

L = lower
M = electric motor
$O2$ = oxygen
U = upper
W = water
(i) = compression or expansion stage i of a compression system

Superscripts

(k) = kth compression system in the air- and gas-supplying network

ACKNOWLEDGMENTS

This work was financially supported jointly by the Brain Korea 21 Project, Korea Energy Management Corporation, and Korea Science and Engineering Foundation (Project R01-2003-000-10697-0). The authors also gratefully acknowledge the technical support provided by Woochang Lee, Euichul Noh, and Kyunghoon Lee of Samsung Petrochemical Corporation, Ulsan, Korea.

ADDRESS

Correspondence concerning this article should be addressed to Professor C. Han, School of Chemical Engineering and Institute of Chemical Processes, Seoul National University, Shillim-dong, Kwanak-gu, Seoul 151-742, South Korea. Tel.: +82-2-880-1887. Fax: +82-2-888-7295. E-mail: chhan@snu.ac.kr

REFERENCES

[1] Han, I.-S. and Han, C., 2003, Modeling of multistage air-compression systems in chemical processes, Ind. Eng. Chem. Res., 42: 2209-2218.

[2] O'Neill, P. A., 1993, Industrial Compressors, Butterworth-Heinemann, Oxford, U.K.

[3] Kroschwitz, J. I., 1991, Encyclopedia of Chemical Technology, John Wiley & Sons, New York, U.S.A.

[4] Lee, W. C., Noh, E. C. and Lee, K. H., 2002, Private communications, Samsung Petrochemical Corporation, Ulsan, Korea.

[5] Rodriguez-Toral, M. A., Morton, W. and Mitchell, D. R., 2001, The use of new SQP methods for the optimization of utility systems, Computers Chem Eng, 25: 287 – 300.

[6] Hui, C.-W. and Natori, Y., 1996, An industrial application using mixed-integer programming technique: a multi-period utility system model, Computers Chem Eng, 20: S1577 – S1582.

[7] Lee, S. J., Lee, M. H., Chang, K. S. and Han, C. Optimization of a utility plant operation based on hierarchical method, HWAHAK KONGHAK, 36: 415 – 421.

[8] Yi, H. S. and Han, C., 2001, The integration of complete replanning and rule based reparing for optimal operation of utility plants, Korean J. Chem Eng, 18: 442 – 450.

[9] Saxena, M. N., 2000, Optimize gas turbine-driven centrifugal compressors, Hydrocarbon Processing, Nov: 61 – 64.

[10] Bloch, H. P., 1996, A Practical Guide to Compressor Technology, McGraw-Hill, New York, U.S.A.

[11] Geladi, P. and Kowalski, B. R., 1986, Partial least-squares regression: A tutorial, Analytica Chimica Acta, 185: 1 – 17.

[12] Rana, S. A. Z., 1985, Understand multistage compressor antisurge control, Hydrocarbon Processing, Mar: 69 – 74.

[13] Rao, S. S., 1996, Engineering optimization-theory and practice, John Wiley & Sons, New York, U.S.A.

[14] Shin, J., Lee, M. and Park S., 1998, Nonlinear static composition estimator for distillation columns using open equation-based nonlinear programming, Korean J. Chem Eng, 15: 667 – 670.